Neurotoxicology 72 (2019) 29–37

Contents lists available at ScienceDirect

Neurotoxicology

journal homepage: www.elsevier.com/locate/neuro

Identification of molecular targets for toxic action by persulfate, an industrial sulfur compound

Takahisa Shimada[a], Kenji Takahashi[a], Makoto Tominaga[b], Toshio Ohta[a,*]

[a] Department of Veterinary Pharmacology, Faculty of Agriculture, Tottori University, Tottori, Japan
[b] Division of Cell Signaling, Okazaki Institute for Integrative Bioscience (National Institute for Physiological Sciences), National Institutes of Natural Sciences, Okazaki, Japan

ARTICLE INFO

Keywords:
Dorsal root ganglia
Heterologous expression
Intracellular Ca^{2+}
Ion channel
Transient Receptor Potential (TRP)
TRPA1
TRPV1
Sensory neuron

ABSTRACT

Persulfate salts are broadly used as industrial chemicals and exposure to them causes occupational asthma, occupational rhinitis and contact dermatitis. However, the mechanisms underlying these toxic actions are not fully elucidated. Transient receptor potential (TRP) vanilloid 1 (V1), ankyrin 1 (A1) and melastatin 8 (M8) are non-selective cation channels preferentially expressing sensory neurons. These channels are known to be involved in respiratory and skin diseases. In the present study, we investigated the effects of sodium persulfate on these TRP channels. In wild-type mouse sensory neurons, persulfate evoked $[Ca^{2+}]_i$ increases that were inhibited by removal of extracellular Ca^{2+} or blockers of TRPA1 but not by those of TRPV1 and TRPM8. Persulfate failed to evoke $[Ca^{2+}]_i$ responses in neurons from TRPA1(-/-) mice, but did evoke them in neurons from TRPV1(-/-) mice. In HEK 293 cells expressing mouse TRPA1 (mTRPA1-HEK), persulfate induced $[Ca^{2+}]_i$ increases. Moreover, in HEK 293 cells expressing mouse TRPV1 (mTRPV1-HEK), a high concentration of persulfate also evoked $[Ca^{2+}]_i$ increases. Similar $[Ca^{2+}]_i$ responses were observed in HEK 293 cells expressing human TRPA1 and human TRPV1. Current responses were also elicited by persulfate in mTRPA1- and mTRPV1-HEK. Analysis using mutated channels revealed that persulfate acted on electrophilic agonist-sensitive cysteine residues of TRPA1, and it indirectly activated TRPV1 due to the external acidification, because of the disappearance of $[Ca^{2+}]_i$ responses in acid-insensitive mTRPV1 mutant. These results demonstrate that persulfate activates nociceptive TRPA1 and TRPV1 channels. It is suggested that activation of these nociceptive channels may be involved in respiratory and skin injuries caused by exposure to this industrial sulfur compound. Thus, selective TRPA1 and TRPV1 channel blockers may be effective to remedy persulfate-induced toxic actions.

1. Introduction

Persulfate salts are low molecular weight sulfur compounds that function as strong oxidants (Devi et al., 2016). They are widely used in various manufacturing processes in the chemical, pharmaceutical, metallurgic, textile, photographic, food, and cosmetic industries (Yawalkar et al., 1999; de Vooght et al., 2010). However, incidents of severe injuries induced by their inhalation and ingestion, or contact with them, have been reported (Baur et al., 1979; Muñoz et al., 2003; Moscato et al., 2010). Workers in the chemical industry suffer from dermatitis, rhinitis, bronchitis and asthma after exposure to dusts of persulfate salts (Baur et al., 1979). Hairdressers contract occupational asthma and contact dermatitis due to hair bleaches containing persulfate salts (Muñoz et al., 2003; Valks et al., 2005). Experimental inhalation of ammonium persulfate induces occupational asthma and occupational asthma associated with occupational rhinitis with nasal eosinophilic inflammation in humans (Moscato et al., 2010). Thus, persulfate salts are considered to cause occupational diseases in workplaces where they are used. In mice intranasally challenged with persulfate salts after sensitization, increases of lymphocyte numbers, cytokine secretion, elevation of the serum IgE level and asthma-like responses are observed (de Vooght et al., 2010; Ollé-Monge et al., 2014; Cruz et al., 2016). These studies suggest that persulfate-induced diseases are mediated by inflammatory and immunological mechanisms. However, the pathophysiological reactions induced by persulfate salts are not well established.

Transient receptor potential (TRP) channels, nonselective cation channels, are involved in various physiological functions (Clapham et al., 2001; Patapoutian et al., 2003; Julius, 2013). TRPA1, TRPV1 and TRPM8 are preferentially expressed in nociceptive sensory neurons

* Corresponding author at: Department of Veterinary Pharmacology, Faculty of Agriculture, Tottori University, Tottori, Japan.
E-mail address: tohta@muses.tottori-u.ac.jp (T. Ohta).

https://doi.org/10.1016/j.neuro.2019.02.003
Received 19 October 2018; Received in revised form 18 January 2019; Accepted 4 February 2019
Available online 06 February 2019
0161-813X/

(Patapoutian et al., 2009) as well as non-neural tissues (Ji et al., 2016). TRPA1 contributes to sensory transduction and responds to a wide variety of pungent natural compounds and environmental irritants (Story et al., 2003; Bandell et al., 2004). TRPV1 is activated by polymodal stimuli such as capsaicin, protons and heat, resulting in pain production (Caterina et al., 1997; Tominaga and Tominaga, 2005). TRPM8 is sensitized by physiologically cool temperatures and cooling compounds (McKemy et al., 2002; Peier et al., 2002) and is related to chemical-induced inflammation (Kim et al., 2017).

TRP channels have been shown to be implicated in the pathogenesis of respiratory and skin diseases (Grace et al., 2014.;Caterina and Pang, 2016). Harmful environmental irritants and industrial pollutants that activate TRPA1 in the airways cause asthma-like symptoms such as cough, wheezing, dyspnea and subsequent hypersensitivity to chemical and physical stimuli (Preti et al., 2012). 2,4-Dinitrochlorobenzene, which is a well-known allergic sensitizer, activates TRPA1 (Saarnilehto et al., 2014). It has been reported that a single exposure to capsaicin causes symptoms like reactive airway dysfunctions syndrome, which is a subtype of occupational asthma (Copeland and Nugent, 2013). TRPM8 expressed in the respiratory airway is associated with cold-induced asthma and its exacerbation (Xing et al., 2008). Menthol is known to cause urticarial asthma and rhinitis (McGowan, 1966; Andersson and Hindsen, 2007). Under some pathological conditions, it has been suggested that neurogenic inflammation is induced by neuropeptides released from sensory neurons through the activation of TRP channels (Grace et al., 2014; Kaneko and Szallasi, 2014; Caterina and Pang, 2016; Gouin et al., 2017). A recent paper shows that drosophila TRPA1 is activated by a persulfate/TEMED mixture (Du et al., 2016). However, the molecular target of persulfate-induced toxicity has remained unknown.

In the present study, we investigated the effects of sodium persulfate on cultured mouse dorsal root ganglion (DRG) neurons and HEK 293 cells heterologously expressing nociceptive TRP channels. To detect channel activity, we used fura-2-based $[Ca^{2+}]_i$ imaging and electrophysiological techniques. The present results revealed that persulfate activated TRPA1 and TRPV1 but not TRPM8. Analyses of the mutant channel suggested that cysteine residues located in the N-terminal internal domain of TRPA1 were related to the sensitivity to persulfate. Since a solution containing persulfate at a high concentration became acidic, it is likely that an indirect acid effect may be involved in the persulfate-induced TRPV1 activation. These results suggest that exposure to persulfate salts causes respiratory and skin diseases via activation of TRPA1 and TRPV1. Therefore, inhibition of these TRP channels may become a novel therapeutic treatment for persulfate-induced occupational disorders.

2. Materials and methods

2.1. Isolation and culture of mouse DRG neurons

All protocols for animal experiments were approved by the Committee on Animal Experimentation of Tottori University. All efforts were made to minimize the number of animals used. Mouse DRG cells were isolated and cultured as described previously (Ogawa et al., 2012). Adult wild-type C57BL/6 mice of either sex (4–12 weeks olds), TRPA1(-/-) mice (kindly provided by Dr. D. Julius, University of California) and TRPV1(-/-) mice of the same strain (The Jackson Laboratory, Bar Harbor, ME, USA) were euthanized with CO_2 gas. Then DRGs were removed and dissected in phosphate-buffered saline (PBS: in mM, 137 NaCl, 10 Na_2HPO_4, 1.8 KH_2PO_4, 2.7 KCl). The isolated ganglia were enzymatically digested for 30 min at 37 °C with collagenase (0.4–1 mg/ml, type II, Worthington, Lakewood, NJ, USA) and DNase I (1 mg/ml, Roche Molecular Biochemicals, Indianapolis, IN, USA). Subsequently, the ganglia were subjected to a second enzymatic digestion in PBS-containing trypsin (10 mg/ml, Sigma, St. Louis, MO, USA) and DNase I (1 mg/ml) for 15 min at 37 °C. After enzyme digestion, the ganglia were washed with the culture medium, Dulbecco's-modified Eagle's medium (DMEM; Sigma) supplemented with 10% fetal bovine serum (FBS; Sigma), penicillin G (100 U/ml) and streptomycin (100 μg/ml). DRG cells were obtained by gentle trituration with a fine-polished Pasteur pipette. Then the cell suspension was centrifuged (800 rpm, 2 min, 4 °C) and the pellet-containing cells were resuspended with the culture medium. Aliquots were placed onto glass coverslips coated with poly-D,L-lysine (Sigma) and cultured in a humidified atmosphere of 95% air and 5% CO_2 at 37 °C. In the experiment, cells cultured within 24 h were used.

2.2. Heterologous expression in HEK 293 cells

Human embryonic kidney (HEK) cells were transfected with 1 μg of mouse TRPA1 (mTRPA1), mouse TRPV1 (mTRPV1), mouse TRPM8 (mTRPM8), a double cysteine mutant of mTRPA1 (C422S/C634S, mTRPA1-2C), mTRPV1 mutants (F660S), human TRPA1 (hTRPA1) or human TRPV1 (hTRPV1) using a transfection reagent (Lipofectamine 2000, Invitrogen). HEK 293 cells were cultured in DMEM supplemented with 10% FBS, 100 U/ml penicillin G and 100 μg/ml streptomycin. For patch-clamp recording, a GFP-expressing vector was cotransfected. Cells were used at 24 h after transfection.

2.3. Measurement of $[Ca^{2+}]_i$

Intracellular Ca^{2+} concentrations ($[Ca^{2+}]_i$) in individual cells were measured with the fluorescent Ca^{2+} indicator fura-2 using a fluorescent-imaging system controlling illumination and acquisition (Aqua Cosmos, Hamamatsu Photonics, Hamamatsu, Japan) as described previously (Ohta et al., 2008). Cells were incubated for 40 min at 37 °C with 10 μM fura-2 AM (Molecular Probes) in HEPES-buffered solution (in mM: 134 NaCl, 6 KCl, 1.2 $MgCl_2$, 2.5 $CaCl_2$, 5 glucose, and 10 HEPES, pH 7.4). A coverslip with fura-2-loaded cells was placed in an experimental chamber set on the stage of a microscope (Olympus IX71) equipped with an image acquisition and analysis system. Cells were illuminated every 5 s with lights at 340 and 380 nm, and the respective fluorescence signals at 500 nm were measured with a charge-coupled device camera (ORCA-ER, Hamamatsu Photonics). The ratios of fluorescent signals (F340/F380) for $[Ca^{2+}]_i$ were calibrated as described previously (Ohta et al., 2008). Cells were continuously perfused with the external solution at a flow rate of ~ 2 ml/min. The composition of high-KCl solution was (in mM) 80 KCl, 60 NaCl, 1.2 $MgCl_2$, 2.5 $CaCl_2$, and 10 HEPES (pH 7.4 with NaOH). For extracellular Ca^{2+}-free HEPES-buffered solution (0Ca), $CaCl_2$ was omitted and EGTA (0.5 mM) was added. To examine the effects of persulfate, we prepared persulfate-containing solutions by simply adding them to the HEPES-buffered solution unless otherwise noted. All experiments were carried out at room temperature (22–25 °C).

2.4. Electrophysiology

Coverslips with HEK 293 cells transfected with each vector were mounted in an experimental chamber and superfused with HEPES-buffered solution as for Ca^{2+} measurement. For membrane current recording, the osmotic pressure-adjusted external solutions were used, since a seal condition became worse resulting in increment of leak currents when using the osmolarity-unadjusted solution. For this, the solutions disolving sodium persulfate at 30 mM, 50 mM and 100 mM, NaCl were reduced to 99 mM, 77 mM and 11 mM, respectively. The pipette solution contained (in mM): 120 KCl, 20 CsOH, 10 HEPES, 10 EGTA, 1.2 MgATP, pH 7.3 with CsOH. The resistance of patch electrodes was 4 ~ 5 MΩ. The whole-cell currents were sampled at 5 kHz and filtered at 1 kHz using a patch-clamp amplifier (Axopatch 200B; Molecular Devices, Sunnyvale, CA) in conjunction with an A/D converter (Digidata 1322 A; Molecular Devices). Membrane potential was clamped at −60 mV and voltage ramps from −80 mV to + 100 mV for

100 ms were applied every 5 s.

2.5. Chemicals

The following drugs were used (vehicle and concentration for stock solution). Allyl isothiocyanate (AITC, dimethyl sulfoxide [DMSO, 1 M]) was from Nakarai (Tokyo, Japan). 2-Aminoethoxydiphenyl borate (2APB, DMSO, 1 M), AMTB hydrochloride (AMTB, DMSO, 0.05 M), capsaicin (ethanol, 1 mM), cremophor EL (distilled water [DW], 1%), HC-030031 (DMSO, 0.1 M), mibefradil (DW, 0.05 M), menthol (DMSO, 1 M) and sodium persulfate were obtained from Sigma. A967079 (DMSO, 0.01 M) was from Focus Biomolecules (Pennsylvania, USA). N-(4-t-butylphenyl)-4-(3-chloropyridin-2-yl) tetrahydropyrazine-1(2 H)-carboxamide (BCTC, DMSO, 0.05 M) was from Biomol Research Laboratories, Inc. (Plymouth Meeting, PA, USA). Persulfate-containing aqueous solutions were made just before each experiment. All other drugs used were of analytical grade.

2.6. Data analysis

Data are presented as the mean ± SEM (n = number of cells). For comparison of two groups, data were analyzed using the unpaired Student's *t*-test. For multiple comparisons, one-way ANOVA following by the Tukey-Kramer test was used. Differences with a P-value of less than 0.05 were considered significant. The average percentage (± SEM) of persulfate-responding cells from mouse DRGs was calculated by division of the number of KCl-responding cells obtained from each coverslip.

3. Results

3.1. $[Ca^{2+}]_i$ responses to persulfate in mouse DRG neurons

In the present study, we used sodium salts of persulfate (Fig. 1A). First, we examined the effects of persulfate on changes in the intracellular Ca^{2+} concentration ($[Ca^{2+}]_i$) in cultured mouse DRG cells. Persulfate elicited $[Ca^{2+}]_i$ increases in some of the cells responding to KCl, but not in non-responding cells (Fig. 1B). Persulfate started to evoke $[Ca^{2+}]_i$ from 10 mM and its magnitude increased in a dose-dependent manner (Fig. 1C). Since the magnitude of the $[Ca^{2+}]_i$ response to persulfate did not plateau even at 100 mM, the 50% effective concentration (EC_{50}) value was not estimated. The percentages of mouse DRG neurons responding to persulfate also increased in a dose-dependent manner. The level of the $[Ca^{2+}]_i$ increase induced by persulfate at 30 mM gradually returned to the original level after its washout (Fig. 1Ba), while that at 100 mM was sustained (Fig. 1Bb). In the following experiment, we mainly used 30 mM persulfate.

3.2. Inhibition of persulfate-induced $[Ca^{2+}]_i$ increases by removal of extracellular Ca^{2+} and TRPA1 blockers

To clarify the source of the $[Ca^{2+}]_i$ increases induced by persulfate, the effect of removal of extracellular Ca^{2+} on the persulfate-induced $[Ca^{2+}]_i$ increase was examined. Persulfate failed to evoke $[Ca^{2+}]_i$ in the absence of external Ca^{2+}, indicating that the persulfate promoted the Ca^{2+} influx in DRG neurons (Fig. 2Ab and 2B). Next, we examined the effect of TRP channel blockers on the $[Ca^{2+}]_i$ responses to persulfate. Both HC-030031 (10 μM) and A967079 (1 μM), TRPA1 blockers, inhibited persulfate-induced $[Ca^{2+}]_i$ increases (Fig. 2Ac and 2B). Neither BCTC (10 μM), a TRPV1 blocker, nor AMTB (10 μM), a TRPM8 blocker, suppressed the persulfate-induced $[Ca^{2+}]_i$ increases (Fig. 2B). It has been reported that sodium hydrogen sulfide, a sulfur-containing H_2S donor, sensitizes T-type Ca^{2+} channels (Matsunami et al., 2009; Takahashi et al., 2010). Although persulfate is a sulfur compound, mibefradil (10 μM), a T-type Ca^{2+} channel blocker did not inhibit persulfate-induced $[Ca^{2+}]_i$ increases. These pharmacological data suggested that the activation of TRPA1 may be involved in the persulfate-induced $[Ca^{2+}]_i$ increase in mouse sensory neurons.

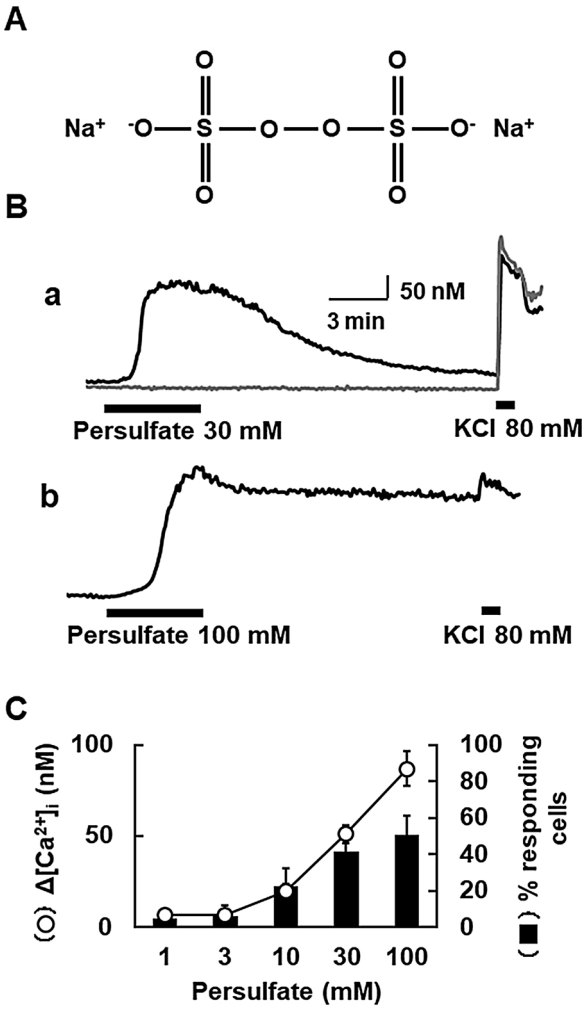

Fig. 1. Persulfate stimulates a subset of mouse DRG neurons. (A) The structural formula of sodium persulfate. (B) Actual recordings of $[Ca^{2+}]_i$ responses to the sequential application of persulfate (a; 30 mM, b; 100 mM) and KCl (80 mM) in mouse DRG cells. (C) Circles and columns show the concentration-response curve for persulfate-induced $[Ca^{2+}]_i$ increases and the percentages of persulfate-responding neurons among all neurons, respectively. The percentages of persulfate-responding cells were calculated from the percentage obtained with each coverslip. Circles and columns with vertical lines show mean ± SEM (n = 36–82, from three mice).

3.3. Persulfate increases $[Ca^{2+}]_i$ in mouse DRG neurons sensitive to a TRPA1 agonist

Next, we examined the relationship between TRP channels and persulfate in mouse DRG neurons. Fig. 3A shows actual traces of changes in $[Ca^{2+}]_i$ in response to persulfate and subsequent allyl isothiocyanate (AITC, a TRPA1 agonist), capsaicin (a TRPV1 agonist) and KCl in mouse DRG neurons. The Venn diagram indicates that most of the persulfate-sensitive neurons were also AITC-sensitive, suggesting that persulfate stimulates mouse DRG neurons expressing TRPA1. To further determine the involvement of TRPA1 in the persulfate-induced $[Ca^{2+}]_i$ increase, we examined the effects of persulfate on DRG neurons from two TRP-deficient mice. In neurons from the TRPV1 (-/-) mouse, $[Ca^{2+}]_i$ responses similar to those in wild-type mouse occurred and the percentages of cells responding to persulfate were almost the same as for AITC (Fig. 3Ab and 3B). In contrast, cells responding to AITC and persulfate disappeared in DRG neurons from the TRPA1(-/-) mouse

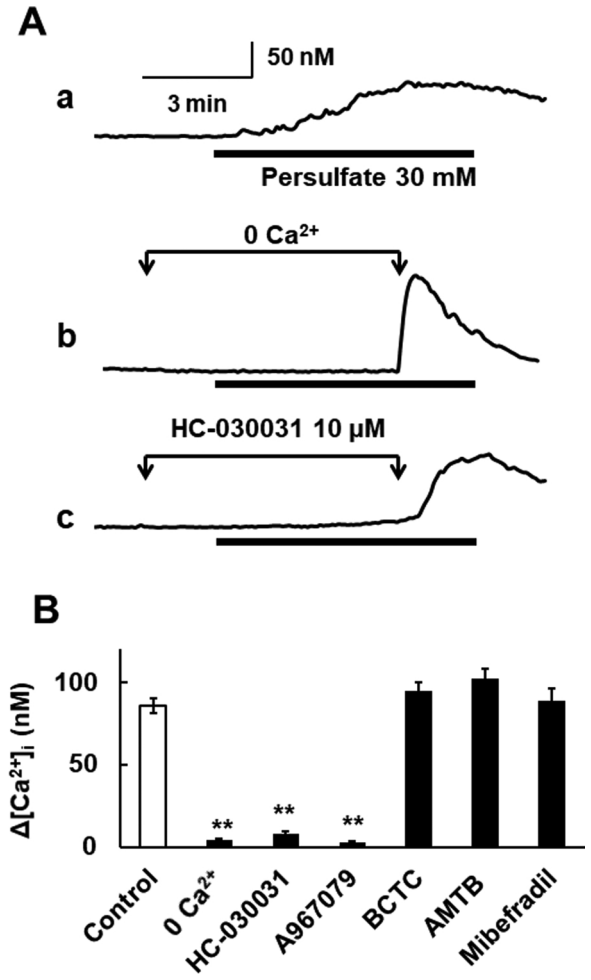

Fig. 2. Inhibition of persulfate-induced $[Ca^{2+}]_i$ increases by removal of extracellular Ca^{2+} and TRPA1 blockers. (A) Actual recordings of $[Ca^{2+}]_i$ responses to persulfate (30 mM) without (a: Control) and with the removal of external Ca^{2+} (b: 0 Ca^{2+}) or a TRPA1 antagonist (c: HC-030031, 10 μM) in mouse DRG neurons. The removal of extracellular Ca^{2+} or the application of HC-030031 was performed 2 min before and for 5 min during the application of persulfate. (B) Summarized effects of the removal of extracellular Ca^{2+} and antagonists for TRPA1 (HC-030031, 10 μM; A967079, 1 μM), TRPV1 (BCTC, 10 μM), TRPM8 (AMTB, 10 μM) and a T-type Ca^{2+} channel blocker (mibefradil, 10 μM). Columns with vertical lines show mean ± SEM (Control; n = 163, 0 Ca^{2+}; n = 37, HC-030031; n = 43, A967079; n = 37, BCTC; n = 76, AMTB; n = 63, mibefradil; n = 54, from three mice). **, P < 0.01 vs. Control, one-way ANOVA with Tukey-Kramer test.

(Fig. 3Ac and 3B). These results clearly indicated that persulfate (30 mM) stimulated TRPA1 channels in mouse sensory neurons.

3.4. $[Ca^{2+}]_i$ responses to persulfate in heterologously expressed TRP channels

As described in the previous section, persulfate preferentially stimulated native TRPA1 channels expressed in mouse sensory neurons. Next, we examined the effect of persulfate on heterologously expressed TRP channels in HEK 293 cells. As shown in Fig. 4Aa, persulfate elicited $[Ca^{2+}]_i$ increases in HEK 293 cells expressing mouse TRPA1 (mTRPA1-HEK). $[Ca^{2+}]_i$ responses to persulfate started at 3 mM and peaked at around 30 mM, and the EC_{50} was estimated to be 8.2 ± 1.4 mM (Fig. 4Ba). HC-030031 (10 μM) attenuated $[Ca^{2+}]_i$ responses to persulfate in mTRPA1-HEK (Fig. 4Ca). Interestingly, persulfate at 100 mM evoked $[Ca^{2+}]_i$ increases in HEK 293 cells expressing mouse TRPV1 (mTRPV1-HEK, Fig. 4Ab and 4B), which were suppressed by BCTC (1 μM, Fig. 4Cb). Since similar $[Ca^{2+}]_i$ responses to persulfate at 30 mM and 100 mM were observed in the osmolality-adjusted solution (data not shown), it is likely that the increment of osmotic pressure was unrelated to the persulfate-induced TRPA1 and TRPV1 activation. Persulfate failed to induce $[Ca^{2+}]_i$ increases in HEK 293 cells expressing mouse TRPM8 (Fig. 4Ba). Like mouse orthologs, human TRPA1 and TRPV1 were also stimulated by persulfate in similar concentration ranges. The EC_{50} value of hTRPA1-HEK was 12.1 ± 0.2 mM (Fig. 4Bb).

When persulfate was dissolved into the HEPES-buffered solution, the pH of the solution gradually decreased. The pH of 30 mM and 100 mM persulfate-containing solution became 7.1 ± 0.02 and 4.8 ± 0.5, respectively. Since rodent TRPA1 is not activated by external acid (De la Roche et al., 2013) and the present study (data not shown), the indirect acidic effects are negligible for persulfate-induced TRPA1 activation. On the other hand, TRPV1 is well-known to be activated by external acid (Tominaga and Tominaga, 2005). Thus, a stimulatory effect of persulfate (100 mM) on TRPV1 seems to be due to the acidic effect as mentioned later (Fig. 6).

As shown in Fig. 4D, mTRPA1-HEK was stimulated with various concentrations of persulfate, and thereafter with AITC (30 μM). After the application of persulfate, the AITC-induced $[Ca^{2+}]_i$ increase significantly decreased depending on the concentration of persulfate at 30 mM or more, indicating that prior administration of persulfate suppressed the following $[Ca^{2+}]_i$ responses to AITC.

3.5. Current responses to persulfate in TRPA1 and TRPV1

To obtain direct evidence for activation of TRPA1 and TRPV1 channels by persulfate, we performed current recording using mTRPA1-HEK and mTRPV1-HEK cells. In these experiments, to minimize the influence of osmotic pressure, the osmolality of persulfate-containing external solutions was adjusted (see Materials and Methods). Fig. 5A and 5B show representative whole-cell currents evoked by persulfate in mTRPA1-HEK and mTRPV1-HEK, respectively. Functional expression of each channel was confirmed by the current responses to AITC (50 μM) and capsaicin (300 nM). The current response to persulfate indicated an outward rectifying current-voltage relationship like those in response to selective agonists (Fig. 5C and 5D). Persulfate-induced current in mTRPA1-HEK and mTRPV1-HEK were suppressed by HC-030031 (10 μM) and BCTC (1 μM), respectively (Fig. 5E and 5F). These results demonstrated that persulfate activated both TRPA1 and TRPV1 channels.

3.6. Molecular mechanisms underlying the persulfate-induced activation of TRPA1 and TRPV1 channels

It has been reported that the activation of TRPA1 by electrophiles occurs through covalent modification of cysteine residues in the N-terminal domain of the channel (Macpherson et al., 2007). Cysteine residue 621 (C621) of human TRPA1 is indicated as a critical site for an electrophilic activation (Bahia et al., 2016) and this amino acid is sufficient to activate TRPA1 by a potent and site-selective electrophilic molecule (Takaya et al., 2015). C621 forms a disulfide bond with C633 via an oxidation by streptozotocin resulting in the TRPA1 activation (Andersson et al., 2015). These reports suggest that interaction between C621 and C633 is important for the activation of TRPA1 by electrophiles. Thus, to determine the molecular mechanism underlying the persulfate-induced TRPA1 activation, we used a mutant mouse TRPA1 channel in which two cysteines (C622, C634; corresponding to C621, C633 of human TRPA1) were substituted for by serines (mTRPA1-2C mutant). As shown in Fig. 6A and 6B, AITC, a typical electrophilic cysteine-modifying agent, failed to evoke the $[Ca^{2+}]_i$ increases in HEK 293 cells expressing the mTRPA1-2C mutant (mTRPA1-2C mutant-HEK). 2-Aminoethoxydiphenyl borate, a non-electrophilic TRPA1 agonist, was capable of activating this mutant channel. Persulfate at 30 mM and 100 mM failed to evoke $[Ca^{2+}]_i$ increases in mTRPA1-2C mutant-

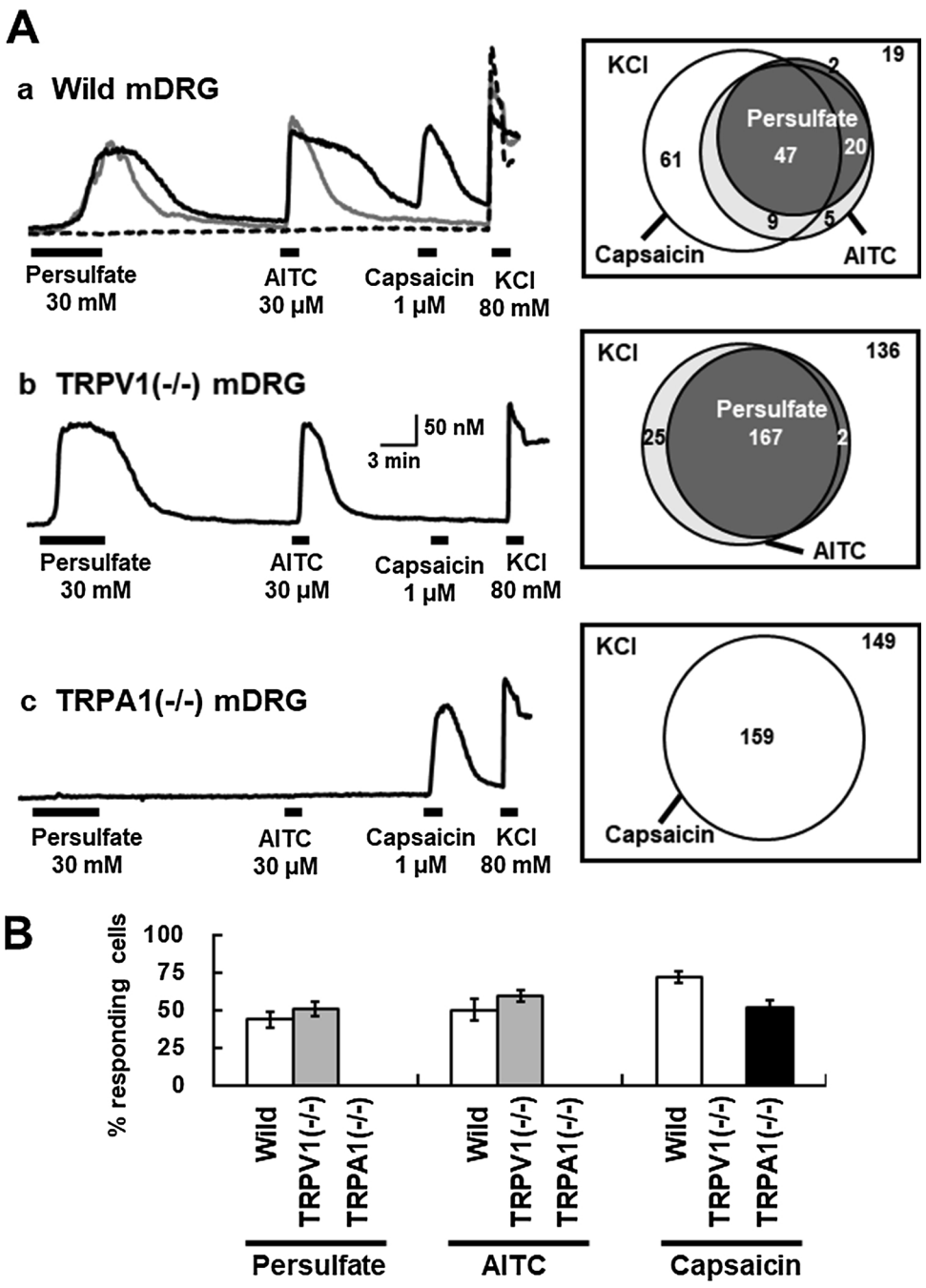

Fig. 3. Persulfate-responding neurons highly correspond to TRPA1 agonist-sensitive ones. (A, left) Actual recordings of $[Ca^{2+}]_i$ responses to the sequential application of persulfate (30 mM), AITC (30 μM), capsaicin (1 μM), and KCl (80 mM) in (a) wild, (b) TRPV1(-/-) and (c) TRPA1(-/-) mouse DRG neurons. (A, right) Venn diagrams showing the sensitivities to persulfate, AITC, capsaicin, and KCl in DRG neurons from three genotype mice. Numbers indicate the number of cells responding to each stimulus. The number in the outermost frame indicates the number of neurons responding to KCl alone. (B) Percentages of cells responding to persulfate, AITC and capsaicin in mouse DRG neurons from each genotype. Columns with vertical lines show mean ± SEM (wild type; n = 163, TRPV1(-/-); n = 330, TRPA1(-/-); n = 308, from three mice for each genotype).

HEK. These data suggested that N-terminal cysteine residues were important for the TRPA1 activation by persulfate.

As mentioned in the previous section, the pH of the solution in which 100 mM persulfate dissolved was gradually decreased to 5.0 or less. When persulfate (100 mM)-containing solution with pH adjusted to neutral was used, no $[Ca^{2+}]_i$ increase occurred (Fig. 6C). Moreover, in HEK 293 cells expressing acid-insensitive mTRPV1 mutant (F660S, Aneiros et al., 2011), persulfate failed to evoke $[Ca^{2+}]_i$ increases (Fig. 6D). Thus, it seems that an indirect acidification is involved in the TRPV1 activation by persulfate at a high concentration.

4. Discussion

Persulfate salts are low molecular weight sulfur compounds that are widely used in various manufacturing processes. It has been reported that persulfate salts cause occupational asthma, occupational rhinitis and contact dermatitis in workplaces via contact (Baur et al., 1979). Several TRP channels such as TRPA1, TRPV1 and TRPM8 are implicated in the pathogenesis and symptoms of respiratory and skin diseases (Grace et al., 2014.;Caterina and Pang, 2016). In the present study, we examined the effects of sodium persulfate on TRPA1, TRPV1 and TRPM8. We demonstrated that persulfate predominantly activated TRPA1 and persulfate at a high dose (100 mM) also activated TRPV1. Our previous report has shown that H_2S and its oxidized product polysulfide, which are endogenous sulfur compounds, also stimulate TRPA1 channels (Ogawa et al., 2012; Hatakeyama et al., 2015). Although, H_2S has been shown to stimulate T-type Ca^{2+} channels (Matsunami et al., 2009; Takahashi et al., 2010), this was not the case for persulfate in mouse DRG neurons because of the ineffectiveness of mibefradil, a T-type Ca^{2+} channel blocker.

Electrophilic TRPA1 activators act on TRPA1 via covalent binding to N-terminal internal cysteine residues of TRPA1 (Hinman et al., 2006;

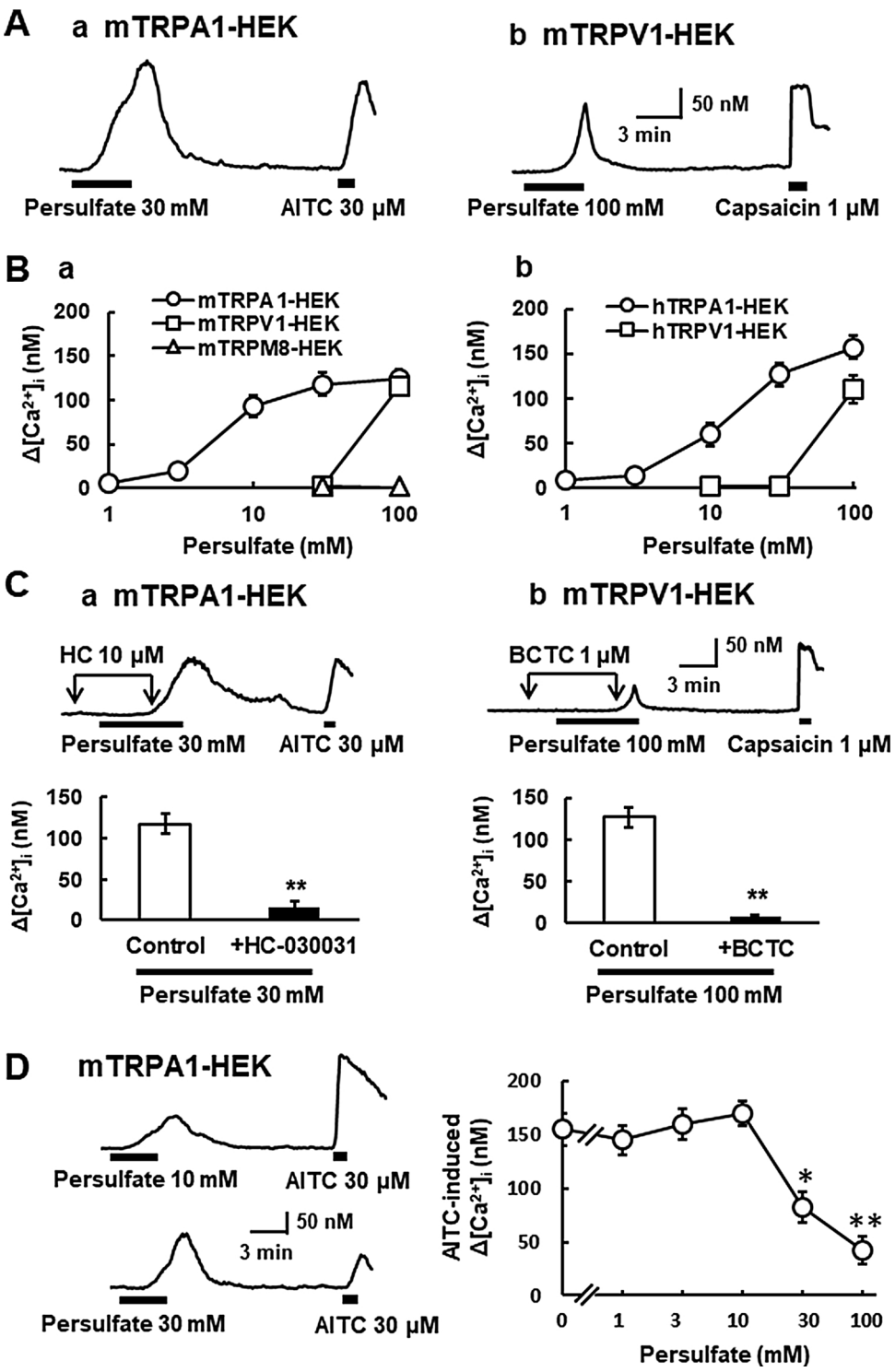

Fig. 4. $[Ca^{2+}]_i$ responses to persulfate in heterologously expressed TRP channels. (A) (a) Actual trace of $[Ca^{2+}]_i$ responses to persulfate (30 mM) and AITC (30 μM) in HEK 293 cells expressing mouse TRPA1 (mTRPA1-HEK) and (b) those to persulfate (100 mM) and capsaicin (1 μM) in HEK 293 cells expressing mouse TRPV1 (mTRPV1-HEK). (B) Concentration-response curves for persulfate-induced $[Ca^{2+}]_i$ increases in (a) mTRPA1-HEK, mTRPV1-HEK and HEK 293 cells expressing mouse TRPM8 (mTRPM8-HEK), and in (b) HEK 293 cells expressing human TRPA1 (hTRPA1-HEK) and human TRPV1 (hTRPV1-HEK). Symbols with vertical lines show mean ± SEM (mTRPA1-HEK; n = 22–38, mTRPV1-HEK; n = 58–82, mTRPM8-HEK; n = 26–38, hTRPA1-HEK; n = 34–57, hTRPV1-HEK; n = 18–24, from three-five different transfections). (C) Actual traces and summarized effects of HC-030031 (10 μM) on persulfate (30 mM)-induced $[Ca^{2+}]_i$ increases in mTRPA1-HEK (a) and those of BCTC (1 μM) on persulfate (100 mM)-induced $[Ca^{2+}]_i$ increases in mTRPV1-HEK (b). Each cell was stimulated with persulfate for 6 min (Control). Application of HC-030031 or BCTC was performed 2 min before and for 4 min during the application of persulfate (a, Control; n = 31, +HC-030031; n = 28, b, Control; n = 82, +BCTC; n = 19, from three-six different transfections). **, P < 0.01 vs. Control. (D) From top to bottom, actual traces of $[Ca^{2+}]_i$ responses to persulfate (10 mM, 30 mM) for 4 min, and AITC (30 μM) for 1 min in mTRPA1-HEK. (E) Summarized effects of persulfate at various concentrations on $[Ca^{2+}]_i$ responses to subsequently applied AITC in mTRPA1-HEK (n = 29–38, from three different transfections). *, P < 0.05, **, P < 0.01 vs 0 mM by one-way ANOVA with Turkey-kramer test.

Macpherson et al., 2007). In the present study, persulfate failed to activate AITC-insensitive cysteine-mutated TRPA1-expressing HEK 293 cells. Furthermore, AITC-induced $[Ca^{2+}]_i$ responses were suppressed in mTRPA1-HEK after the application of persulfate in a concentration-dependent manner. These results indicate that activation sites for persulfate may be consistent with those for AITC. Oxidative stresses and oxidants, including hydrogen peroxide, are also reported to activate TRPA1 via the modulation of cysteine residues (Andersson et al., 2008; Sawada et al., 2008; Takahashi et al., 2008). Since persulfate is a stronger oxidant than hydrogen peroxide, it might oxidize them to activate TRPA1 like hydrogen peroxide (Huang et al., 2002). The low sensitivity to persulfate of TRPA1 may be attributed to its lower permeability to intracellular sites.

Although TRPV1 and TRPA1 are sensitive to an osmotic increase (Zhang et al., 2008; Nishihara et al., 2011), the osmotic pressure-adjusted solution containing persulfate could still elicit $[Ca^{2+}]_i$ (data not shown) and current responses in mTRPV1- and mTRPA1-HEK (Fig. 5). Therefore, the osmotic increase was not related to the persulfate-induced activation of TRPA1 and TRPV1. It is known that acid activates TRPV1 (Tominaga and Tominaga, 2005). When sodium persulfate (100 mM) was dissolved into HEPES-buffered solution, the pH of the solution was gradually decreased to 5.0 or less. When using pH-adjusted

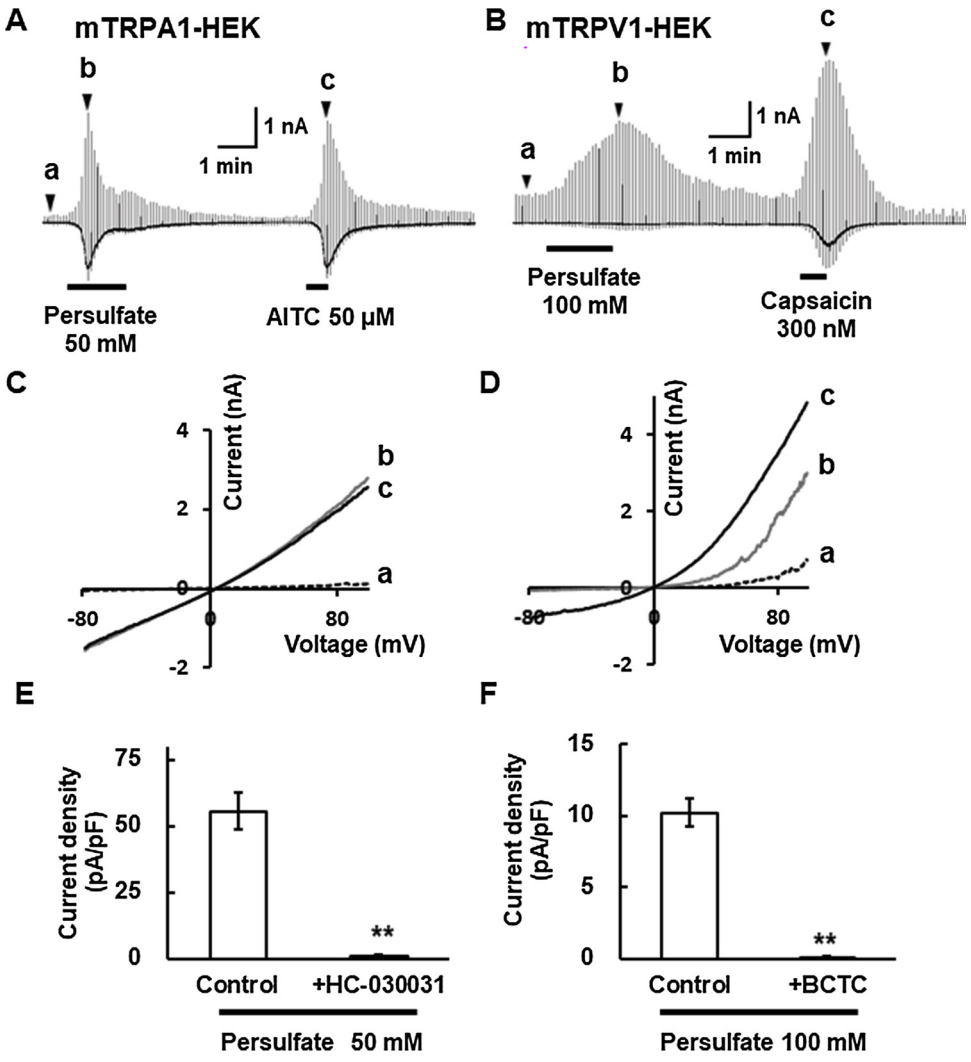

Fig. 5. Current responses to persulfate in HEK 293 cells expressing mTRPA1 and mTRPV1 (A) Representative trace of whole-cell currents elicited by persulfate (50 mM) followed by AITC (50 μM) in mTRPA1-HEK and (B) that by persulfate (100 mM) followed by capsaicin (300 nM) in mTRPV1-HEK. (C) The current-voltage (I–V) curves for before (a) and after the application of persulfate (b) and AITC (c) in mTRPA1-HEK, and (D) those for before (a) and after application of persulfate and capsaicin (c) in mTRPV1-HEK. (E, F) Summarized effects of HC-030031 (E; 10 μM) and BCTC (F; 1 μM) on the amplitude of the persulfate-induced current in mTRPA1-HEK and mTRPV1-HEK, respectively. Cells were stimulated with persulfate for 90 s (Control) and each blocker was applied 1 min before, during 90 s and after 2 min application of persulfate. Columns with vertical lines show mean ± SEM (E; Control; n = 6, +HC-030031; n = 5, F; Control; n = 6, +BCTC; n = 5, from four different transfections). **, P < 0.01 vs Control, Student's *t*-test.

persulfate-containing solution to neutral and in HEK 293 cells expressing pH-insensitive TRPV1 mutant, $[Ca^{2+}]_i$ responses were disappeared (Fig. 6C and 6D). Thus, it is likely that an indirect acidification is involved in the TRPV1 activation by persulfate.

TRPA1 and TRPV1 have species-specific sensitivities to certain agents (Jordt and Julius, 2002; Bianchi et al., 2012; Banzawa et al., 2014). Persulfate elicited $[Ca^{2+}]_i$ increases in the heterologously expressed hTRPA1 and hTRPV1, and their activity concentration ranges were similar to those of the mouse orthologues. Therefore, there was no species difference of the sensitivity to persulfate for TRPA1 and TRPV1 between the mouse and human. In other words, the toxic effects of persulfate are elicited via human TRPA1 and TRPV1 channels.

In this study, we used 1–100 mM sodium persulfate. Some commercial hair bleach agents contain about 200 mM persulfate salts (Jeong et al., 2010). In the case of acute persulfate exposure such as an inhalation and contact, persulfate at such a concentration would sufficiently activate TRPA1 and TRPV1 according to our present results. It has been shown that lymphocytes from ammonium persulfate-sensitized mice secrete interleukin-13 (IL-13), which is associated with atopic dermatitis, after a second stimulation with ammonium persulfate (de Vooght et al., 2010). It is also reported that IL-13 enhances the growth of dermal neuropeptide-secreting afferent nerve fibers, and that TRPA1 is expressed in dorsal root ganglia and mast cells (Oh et al., 2013). Thus, persulfate salts may not only directly activate TRPA1 but also indirectly upregulate TRPA1 expression, resulting in the aggravation of persulfate-related diseases.

The activation of primary sensory neurons triggers the subsequent release of inflammatory neuropeptides, including substance P and calcitonin gene-related peptide (Geppetti et al., 2008). It has been reported that TRPV1 and TRPA1 promote neurogenic inflammation in the skin and airway (Geppetti et al., 2014; Gouin et al., 2017). Persulfate may cause neurogenic inflammation via activation of both channels on the terminals of sensory neurons innervated in skin and airway organs. Furthermore, functional TRPA1 and TRPV1 expression has also been reported in non-neuronal cells of lung and skin tissues that release IL-8, a neutrophil chemoattractant, via their responses to TRPA1 and TRPV1 agonists and contribute to lung inflammation (Nassini et al., 2012; Caterina, 2014; de Logu et al., 2016). An increment in the number of neutrophils has been shown in ammonium persulfate-sensitized mice (Ollé-Monge et al., 2014). Therefore, not only non-neuronal but also neuronal TRPA1 and TRPV1 may be involved in the toxicity of persulfate.

In conclusion, the present data show that persulfate salt activates TRPA1 and TRPV1. To the best of our knowledge, this is the first study to suggest that persulfate-induced diseases are mediated via a neuronal mechanism in addition to well-recognized immunological mechanisms. Thus, TRPA1 and TRPV1 may be promising therapeutic targets for persulfate-induced respiratory and skin failures.

Conflict of interest statement

We have no conflict-of-interest to declare.

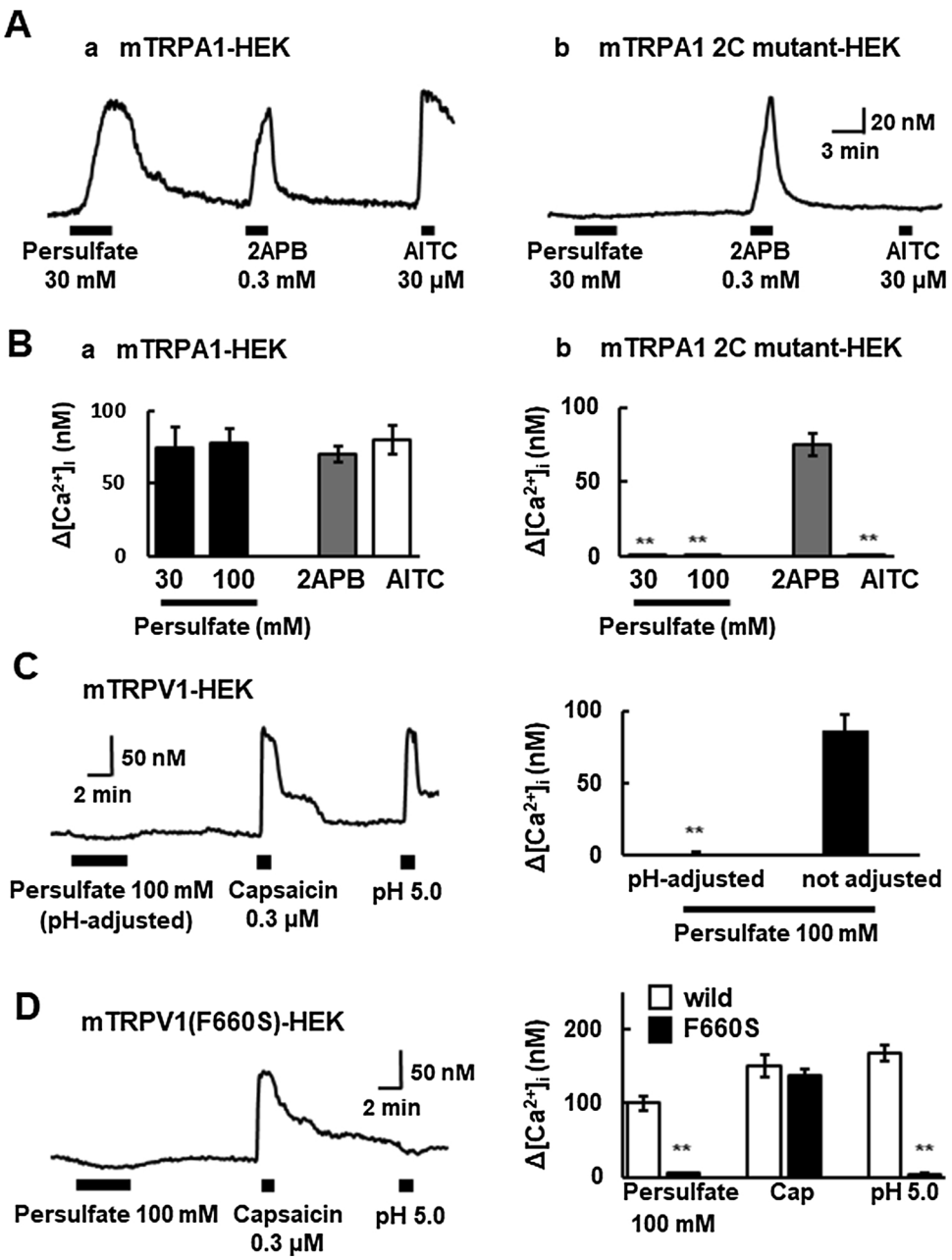

Fig. 6. Involvement of cysteine residues of TRPA1 channel in persulfate-induced TRPA1 channel activation and indirect activation of TRPV1 due to acidification by persulfate at high concentration. (A) Actual traces of $[Ca^{2+}]_i$ responses to the sequential application of persulfate (30 mM), 2-aminoethoxydiphenyl borate (2APB, 300 μM) and AITC (30 μM) in mTRPA1-HEK and HEK 293 cells expressing mouse TRPA1 mutated with two cysteine residues (mTRPA1-2C mutant-HEK). (B) $[Ca^{2+}]_i$ increments induced by persulfate (30 mM, 100 mM), 2APB (300 μM) and AITC (30 μM) in mTRPA1-HEK and mTRPA1-2C mutant-HEK. Columns with vertical lines show mean ± SEM (mTRPA1; n = 39–55, mTRPA1-2C; n = 19–28, from three separate transfections). **, $P < 0.01$ vs. $\Delta[Ca^{2+}]_i$ induced by each drug in mTRPA1-HEK, Student's *t*-test. (C) Actual trace of $[Ca^{2+}]_i$ response to persulfate (100 mM), the solution of which pH was adjusted to neutral (pH-adjusted) in mTRPV1-HEK. Columns with vertical lines show mean ± SEM (pH-adjusted; n = 48, not adjusted; (n = 51), from three different transfections). **, $P < 0.01$ vs. pH not adjusted, Student's *t*-test. (D) Actual trace of $[Ca^{2+}]_i$ response to persulfate (100 mM) in mTRPV1(F660S)-HEK. Columns with vertical lines show mean ± SEM (wild; n = 62, F660S; n = 42, from three different transfections). **, $P < 0.01$ vs. wild, Student's *t*-test.

Roles of authors

TO designed the study; TS conducted experiments; MT conducted data analyses; TS, KT and TO wrote the manuscript.

Acknowledgment

This work was supported, in whole or part, by JSPS KAKENHI (Grant No. 18H02345, T.O).

References

Andersson, M., Hindsen, M., 2007. Rhinitis because of toothpaste and other menthol-containing products. Allergy 62, 336–337.

Andersson, D.A., Gentry, C., Moss, S., Bevan, S., 2008. Transient receptor potential A1 is a sensory receptor for multiple products of oxidative stress. J. Neurosci. 28, 2485–2494.

Andersson, D.A., Filipović, M.R., Gentry, C., Eberhardt, M., Vastani, N., Leffler, A., Reeh, P., Bevan, S., 2015. Streptozotocin Stimulates the Ion Channel TRPA1 Directly: involvement of peroxynitrite. J. Biol. Chem. 290, 15185–15196.

Aneiros, E., Cao, L., Papakosta, M., Stevens, E.B., Phillips, S., Grimm, C., 2011. The biophysical and molecular basis of TRPV1 proton gating. EMBO J. 30, 994–1002.

Bahia, P.K., Parks, T.A., Stanford, K.R., Mitchell, D.A., Varma, S., Stevens Jr, S.M., Taylor-Clark, T.E., 2016. The exceptionally high reactivity of Cys 621 is critical for electrophilic activation of the sensory nerve ion channel TRPA1. J. Gen. Physiol. 147, 451–465.

Bandell, M., Story, G.M., Hwang, S.W., Viswanath, V., Eid, S.R., Petrus, M.J., Earley, T.J., Patapoutian, A., 2004. Noxious cold ion channel TRPA1 is activated by pungent compounds and bradykinin. Neuron 41, 849–857.

Banzawa, N., Saito, S., Imagawa, T., Kashio, M., Takahashi, K., Tominaga, M., Ohta, T., 2014. Molecular basis determining inhibition/activation of nociceptive receptor TRPA1 protein. J. Biol. Chem. 289, 31927–31939.

Baur, X., Fruhmann, G., Liebe, V.V., 1979. Occupational asthma and dermatitis after exposure to dust of persulphate salts in two industrial workers. Respiration 38, 144–150.

Bianchi, B.R., Zhang, X.F., Reilly, R.M., Kym, P.R., Yao, B.B., Chen, J., 2012. Species comparison and pharmacological characterization of human, monkey, rat, and mouse TRPA1 channels. J. Pharmacol. Exp. Ther. 341, 360–368.

Caterina, M.J., 2014. TRP channel cannabinoid receptors in skin sensation, homeostasis and inflammation. ACS Chem. Neurosci. 5, 1107–1116.

Caterina, M.J., Pang, Y., 2016. TRP channels in skin biology and pathophysiology. Pharmaceuticals 9, 77.

Caterina, M.J., Schumacher, M.A., Tominaga, M., Rosen, T.A., Levine, D., Julius, D., 1997. The capsaicin receptor: a heat-activated ion channel in the pain pathway.

Nature 389, 816–824.
Clapham, D.E., Runnels, L.W., Stübing, C., 2001. The TRP ion channel family. Nat. Rev. Neurosci. 2, 387–396.
Copeland, X., Nugent, K., 2013. Persistent respiratory symptoms following prolonged capsaicin exposure. Int. J. Occup. Environ. Med. 4, 211–215.
Cruz, M.J., Olle-Monge, M., Vanoirbeek, J.A., Assialioui, A., Gomez-Olles, S., Muñoz, X., 2016. Persistence of respiratory and inflammatory responses after dermal sensitization to persulfate salts in a mouse model of non-atopic asthma. Allergy Asthma Clin. Immunol. 12, 26.
De la Roche, J., Eberhardt, M.J., Klinger, A.B., Stanslowsky, N., Wegner, F., Koppert, W., Reeh, P.W., Lampert, A., Fischer, M.J., Leffler, A., 2013. The molecular basis for species-specific activation of human TRPA1 protein by protons involves poorly conserved residues within transmembrane domains 5 and 6. J. Biol. Chem. 288, 20280–20292.
De Logu, F., Patacchini, R., Fontana, G., Geppetti, P., 2016. TRP functions in the bronchopulmonary system. Semin. Immunopathol. 38, 321–329.
De Vooght, V., Cruz, M.J., Haenen, S., Wijnhoven, K., Muñoz, X., Hoet, P.M., Morell, F., Nemery, B., Vanoirbee, J.A., 2010. Ammonium persulfate can initiate an asthmatic response in mice. Asthma 65, 252–257.
Devi, P., Das, U., Dalai, A.K., 2016. In-situ chemical oxidation: principle and applications of peroxide and persulfate treatments in wastewater systems. Sci. Total Environ. 571, 643–657.
Du, E.J., Ahn, T.J., Wen, X., Seo, D.W., Na, D.L., Kwon, J.Y., Choi, M., Kim, H.W., Cho, H., Kang, K., 2016. Nucleophile sensitivity of Drosophila TRPA1 underlies light-induced feeding deterrence. Elife, e18425.
Geppetti, P., Nassini, R., Materazzi, S., Benemei, S., 2008. The concept of neurogenic inflammation. BJU Int. 101 (Suppl 3), 2–6.
Geppetti, P., Patacchini, R., Nassini, R., 2014. Transient receptor potential channels and occupational exposure. Curr. Opin. Allergy Clin. Immunol. 14, 77–83.
Gouin, O., L'Herondelle, K., Lebonvallet, N., Gall-Ianotto, C.L., Sakka, M., Buhé, V., Plée-Gautier, E., Carré, J.L., Lefeuvre, L., Misery, L., Garrec, R.L., 2017. TRPV1 and TRPA1 in cutaneous neurogenic and chronic inflammation: pro-inflammatory response induced by their activation and their sensitization. Protein Cell 8, 644–661.
Grace, M.S., Baxter, M., Dubuis, E., Birrell, M.A., Belvisi, M.G., 2014. Transient receptor potential (TRP) channels in the airway: role in airway disease. Br. J. Pharmacol. 171, 2593–2607.
Hatakeyama, Y., Takahashi, K., Tominaga, M., Kimura, H., Ohta, T., 2015. Polysulfide evokes acute pain through the activation of nociceptive TRPA1 in mouse sensory neurons. Mol. Pain 11, 24.
Hinman, A., Chuang, H.H., Bautista, D.M., Julius, D., 2006. TRP channel activation by reversible covalent modification. Proc. Natl. Acad. Sci. U. S. A. 103, 19564–19568.
Huang, K.C., Couttenye, R.A., George, E., Hoag, G.E., 2002. Kinetics of heat-assisted persulfate oxidation of methyl tert-butyl ether (MTBE). Chemosphere 49, 413–420.
Jeong, M.S., Lee, C.M., Jeong, W.J., Kim, S.J., Lee, K.Y., 2010. Significant damage of the skin and hair following hair bleaching. J. Dermatol. 37, 882–887.
Ji, R.R., Chamessian, A., Zhang, Y.Q., 2016. Pain regulation by non-neuronal cells and inflammation. Science 354, 572–577.
Jordt, S.E., Julius, D., 2002. Molecular basis for species-specific sensitivity to "hot" chili peppers. Cell 108, 421–430.
Julius, D., 2013. TRP channels and pain. Annu. Rev. Cell Dev. Biol. 29, 355–384.
Kaneko, Y., Szallasi, A., 2014. Transient receptor potential (TRP) channels: a clinical perspective. Br. J. Pharmacol. 171, 2474–2507.
Kim, J.H., Jang, Y.S., Jang, S.H., Jung, K.S., Kim, S.H., Ye, Y.M., Park, H.S., 2017. Toluene diisocyanate exposure induces airway inflammation of bronchial epithelial cells via the activation of transient receptor potential melastatin 8. Exp. Mol. Med. 49, e299.
Macpherson, L.J., Dubin, A.E., Evans, M.J., Marr, F., Schultz, P.G., Cravatt, B.F., 2007. Noxious compounds activate TRPA1 ion channels through covalent modification of cysteines. Nature 445, 541–545.
Matsunami, M., Tarui, T., Mitani, K., Nagasawa, K., Fukushima, O., Okubo, K., Yoshida, S., Takemura, M., Kawabata, A., 2009. Luminal hydrogen sulfide plays a pronociceptive role in mouse colon. Gut 58, 751–761.
McGowan, E.M., 1966. Menthol urticarial. Arch. Dermatol. 94, 62–63.
McKemy, D.D., Neuhausser, W.M., Julius, D., 2002. Identification of a cold receptor reveals a general role for TRP channels in thermosensation. Nature 416, 52–58.
Moscato, G., Pala, G., Perfetti, L., Frascaroli, M., Pignatti, P., 2010. Clinical and inflammatory features of occupational asthma caused by persulphate salts in comparison with asthma associated with occupational rhinitis. Allergy 65, 784–790.
Muñoz, X., Cruz, M.J., Orriols, R., Bravo, C., Espuga, M., Morell, F., 2003. Occupational asthma due to persulfate salts. Chest 123, 2124–2129.
Nassini, R., Pedretti, P., Moretto, N., Fusi, C., Carnini, C., 2012. Transient receptor potential ankyrin 1 channel localized to non-neuronal airway cells. Promotes non-neurogenic inflammation. PLoS One 7, e42454.
Nishihara, E., Hiyama, T.Y., Noda, M., 2011. Osmosensitivity of transient receptor potential vanilloid 1 is synergistically enhanced by distinct activating stimuli such as temparature and protons. PLoS One 6, e22246.
Ogawa, H., Takahashi, K., Miura, S., Imagawa, T., Saito, S., Tominaga, M., Ohta, T., 2012. H_2S functions as a nociceptive messenger through transient receptor potential ankyrin 1 (TRPA1) activation. Neuroscience 218, 335–343.
Oh, M.H., Oh, S.Y., Lu, J., Lou, H., Myers, A.C., Zhu, Z., Zheng, T., 2013. TRPA1-dependent pruritus in IL-13–induced chronic atopic dermatitis. J. Immunol. 191, 5371–5382.
Ohta, T., Imagawa, T., Ito, S., 2008. Novel gating and sensitizing mechanism of capsaicin receptor (TRPV1): tonic inhibitory regulation of extracellular sodium through the external protonation sites on TRPV1. J. Biol. Chem. 283, 9377–9387.
Ollé-Monge, M., Muñoz, X., Vanoirbeek, J.A.J., Gómez-Ollés, S., Morell, F., Cruz, M.J., 2014. Persistence of asthmatic response after ammonium persulfate-induced occupational asthma in mice. PLoS One 9, e109000.
Patapoutian, A., Peier, A.M., Story, G.M., Viswanath, V., 2003. ThermoTRP channels and beyond: mechanisms of temperature sensation. Nat. Rev. Neurosci. 4, 529–539.
Patapoutian, A., Tate, S., Woolf, C.J., 2009. Transient receptor potential channels: targeting pain at the source. Nat. Rev. Drug Discov. 8, 55–68.
Peier, A.M., Moqrich, A., Hergarden, A.C., Reeve, A.J., Andersson, D.A., Story, G.M., Earley, T.J., Dragoni, I., McIntyre, P., Bevan, S., Patapoutian, A., 2002. A TRP channel that senses cold stimuli and menthol. Cell 108, 705–715.
Preti, D., Szallasi, A., Patacchini, R., 2012. TRP channels as therapeutic targets in airway disorders: a patent review. Expert Opin. Ther. Pat. 22, 663–695.
Saarnilehto, M., Chapman, H., Savinko, T., Lindstedt, K., Lauerma, A.I., Koivisto, A., 2014. Contact sensitizer 2,4-dinitrochlorobenzene is a highly potent human TRPA1 agonist. Allergy 69, 1424–1427.
Sawada, Y., Hosokawa, H., Matsumura, K., Kobayashi, S., 2008. Activation of transient receptor potential ankyrin 1 by hydrogen peroxide. Eur. J. Neurosci. 27, 1131–1142.
Story, G.M., Peier, A.M., Reeve, A.J., Eid, S.R., Mosbacher, J., Hricik, T.R., Earley, T.J., Hergarden, A.C., Andersson, D.A., Hwang, S.W., McIntyre, P., Jegla, T., Bevan, S., Patapoutian, A., 2003. ANKTM1, a TRP-like channel expressed in nociceptive neurons, is activated by cold temperatures. Cell 112, 819–829.
Takahashi, N., Mizuno, Y., Kozai, D., Yamamoto, S., Kiyonaka, S., Shibata, T., 2008. Molecular characterization of TRPA1 channel activation by cysteine-reactive inflammatory mediators. Channels 2, 287–298.
Takahashi, T., Aoki, Y., Okubo, K., Maeda, Y., Sekiguchi, F., Mitani, K., Nishikawa, H., Kawabata, A., 2010. Upregulation of Cav3.2 T-type calcium channels targeted by endogenous hydrogen sulfide contributes to maintenance of neuropathic pain. Pain 150, 183–191.
Takaya, J., Mio, K., Shiraishi, T., Kurokawa, T., Otsuka, S., Mori, Y., Uesugi, M., 2015. A potent and site-selective agonist of TRPA1. J. Am. Chem. Soc. 137, 15859–15864.
Tominaga, M., Tominaga, T., 2005. Structure and function of TRPV1. Eur. J. Appl. Physiol. Occup. Physiol. 451, 143–150.
Valks, R., Conde-Salazar, L., Malfeito, J., 2005. Contact dermatitis in hairdressers, 10 years later: patch-test results in 300 hairdressers (1994 to 2003) and comparison with previous study. Dermatitis 16, 28–31.
Xing, H., Ling, J.X., Chen, M., Johnson, R.D., Tominaga, M., Wang, C.Y., Gu, J., 2008. TRPM8 mechanism of autonomic nerve response to cold in respiratory airway. Mol. Pain 4, 22.
Yawalkar, N., Helbling, A., Pichler, C.E., 1999. T cell involvement in persulfate triggered occupational contact dermatitis and asthma. Ann. Allergy Asthma Immunol. 82, 401–404.
Zhang, X.F., Chen, J., Faltynek, C.R., Moreland, R.B., Neelands, T.R., 2008. Transient receptor potential A1 mediates an osmotically activated ion channel. Eur. J. Neurosci. 27, 605–611.